

Inhibition of *O*-GlcNAcase by PUGNAc is dependent upon the oxime stereochemistry

Melissa Perreira,^a Eun Ju Kim,^b Craig J. Thomas^{a,*} and John A. Hanover^b

^aChemical Biology Core Facility, National Institute of Diabetes and Digestive and Kidney Disorders, National Institutes of Health, Bethesda, MD 20892, USA

^bLaboratory of Cell Biochemistry and Biology, National Institute of Diabetes and Digestive and Kidney Disorders, National Institutes of Health, Bethesda, MD 20892, USA

Received 21 July 2005; revised 1 September 2005; accepted 2 September 2005
Available online 7 October 2005

Abstract—The potent *O*-GlcNAcase inhibitor PUGNAc was synthesized and two isomers based on the *E* and *Z* stereochemistry of the oxime moiety were separated, defined, and tested for activity. Several lines of evidence were examined in an effort to define the correct stereochemical assignments of each form of PUGNAc. The ability of the *Z* stereoisomer to undergo the Beckmann rearrangement was ultimately the most definitive proof. It was determined via both in vitro and intact cell experiments that the *Z* form of PUGNAc was vastly more potent an inhibitor of *O*-GlcNAcase than the *E* form.
© 2005 Elsevier Ltd. All rights reserved.

1. Introduction

Among the assorted post-translational modifications of nuclear and cytoplasmic proteins are O-linked *N*-acetylglucosamine (*O*-GlcNAc) addition and removal on serine and threonine residues by *O*-GlcNAc transferase and *O*-GlcNAcase, respectively.¹ The adornment of *O*-GlcNAc upon protein surfaces has been suggested to take part in a functional interplay involving both kinases and phosphatases with implications on cellular signaling and regulation.² Disruptions of these multifaceted interactions likely have consequences in maladies including diabetes mellitus and cellular events such as apoptosis. Conversely, manipulation of these pathways could provide a significant advantage within the management of numerous diseases.

There are many potent and selective small molecule inhibitors and activators for the assorted protein phosphatases and, in particular, kinases. The development of selective activators or inhibitors of *O*-GlcNAcase (EC 3.2.1.52) and *O*-GlcNAc transferase (EC 2.4.1.94) remains minuscule by comparison. Currently, the only

well-characterized inhibitor of *O*-GlcNAc transferase is Alloxan (**1**) (Fig. 1).³ Additionally, there are few known inhibitors of *O*-GlcNAcase including streptozotocin (**2**) and *O*-(2-acetamido-2-deoxy- β -D-glucopyranosylidene)amino-*N*-phenylcarbamate (PUGNAc) (**3**).⁴

PUGNAc was initially noted for its potent inhibition of β -*N*-acetylglucosaminidases and it was suggested that inhibition was the result of substrate mimicry.^{4a} Composed of a hydroximolactone *N*-acetyl triol moiety, PUGNAc does indeed mimic the structure of native glucosamine substrates such as UDP-GlcNAc (**4**). The ability of PUGNAc to mimic several glucosamine substrates undoubtedly plays a role in its inhibition of *O*-GlcNAcase and could be a useful reagent in delineating the phenotypical response to exaggerated levels of O-linked *N*-acetylglucosamine modifications of proteins. Recently, it has been reported that prolonged cellular exposure to PUGNAc has resulted in the amplified incidence of *O*-GlcNAc incorporation to proteins and an ensuing resistance to insulin.⁵ While the elucidation of the biochemical potential of PUGNAc continues to receive attention, complete understanding of the role of the oxime stereochemistry of PUGNAc has been largely ignored. Herein we synthesize, isolate, and define each of the PUGNAc isomers and show that the ability of PUGNAc to inhibit the action of *O*-GlcNAcase is dependent upon the stereochemistry of the oxime.

Keywords: PUGNAc; *O*-GlcNAcase; Oxime stereochemistry.

* Corresponding author. Tel.: +1 301 496 40761; fax: +1 301 402 0008; e-mail: craigj@niddk.nih.gov

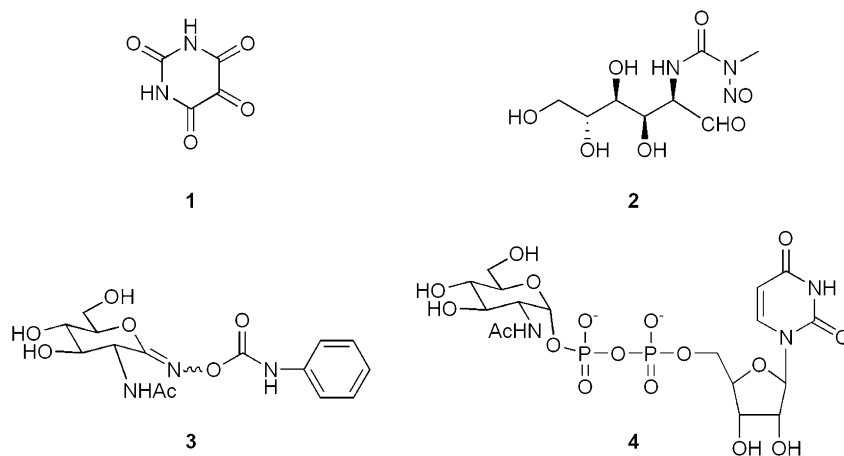


Figure 1. Structures of alloxane (1), streptozocin (2), PUGNAc (3), and UDP-GlcNAc (4).

2. Results

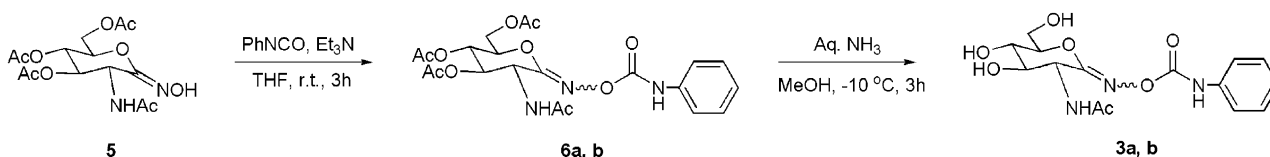
2.1. Chemistry

Synthetic elucidation of PUGNAc was accomplished employing the original pathway developed by Vasella and co-workers.⁶ Following the coupling of the hydroximolactone (**5**) with phenyl isocyanate to form the corresponding phenylcarbamoyl (**6**) (Scheme 1), we noted the presence of two products by TLC and HPLC. The separation of each isomer was difficult by flash chromatography, however, their isolation by HPLC proved uncomplicated. The two isomers of **6a** and **6b** were formed in approximately a 5:2 ratio based upon HPLC integration and comparison of the NMR integration of corresponding peaks from an aliquot of the principal product mixture. The original product mixture of **6** was utilized in the subsequent deacetylation reaction to produce **3a** and **3b**, and we found that the product ratio was maintained based upon HPLC integration. Following purification of the two isomers **6a** and **6b**, aliquots of each were treated with ammonia to effect deacetylation and it was verified based upon HPLC retention time alignment that the oxime stereochemistry was unchanged during deacetylation. Previously, the isolation of PUGNAc relied upon flash chromatography and a subsequent crystallization to yield a single isomer. PUGNAc has been generally referred to as the *Z* isomer, although we are unaware of any crystallographic evidence or NMR correlations that would allow exact stereochemical definition.

Given the plethora of data concerning the importance of lock and key models for ligand–protein interactions, the biochemical relationship between the two structures of

PUGNAc seemed important to determine. Following HPLC separation of the two isomers of PUGNAc, we set out to determine their absolute stereochemistry. We initially designated the stereoisomers based upon their HPLC elution times; for example, as the “F” or fast-running isomer and the “S” or slow-running isomer. Following several failed attempts to produce acceptable crystals for X-ray analysis of either the “F” or “S” isomers of PUGNAc, we concluded that the designation of the absolute stereochemistry by other means would be necessary. We explored several established lines of evidence including melting point comparisons, compound stability, and NMR spectral shifts with limited success due to inconsistencies between oxime and hydroximolactone structures and lack of precedence in the case of hydroximolactones. Ultimately, the most straightforward line of evidence was the capability of the *Z* isomer of PUGNAc to undergo the Beckmann rearrangement. Finally, the “F” PUGNAc was designated as the *Z* stereoisomer (**3a**) and the “S” PUGNAc was the *E* stereoisomer (**3b**) (Fig. 2).

Several inferences can be made based upon the experimental evidence such as melting points and molecular stability.⁷ However, these reports are often in disagreement with one another based upon the specific structural elements of the oxime and/or hydroximolactone. For example, several studies of oximes and hydroximolactones suggest that the *E* stereoisomer is more stable than its *Z* counterparts,^{7b,d} while others present evidence that the *Z* isomers of oximes or hydroximolactones are the more robust.^{7a,c,e,f} In our hands, the *Z* isomer (**3a**) of PUGNAc decomposed completely in a 0.1% trifluoroacetic acid aqueous solution after only 8 h, while the *E* isomer (**3b**) remained intact up to and exceeding 7 days.



Scheme 1.

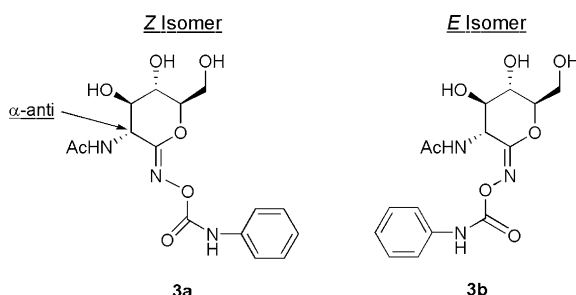


Figure 2. Structural dissimilarity of the *E* and *Z* isomers of PUGNAc.

Further, the *Z* isomer was seen to decompose in neutral conditions (1:1 solution of H₂O and CH₃CN) over a period of 5 weeks, while the *E* isomer, again, remained whole. The same trend was noticed in the peracetylated analogues (**6a** and **6b**).

Melting point variations have been used as determinants of stereochemistry as well. Several studies suggest that *Z* oximes will generally have lower melting points than *E* oximes.^{7a,c,e,f} Again, there are studies suggesting just the opposite.^{7b,e} Researchers point to several explanations and have often invoked the use of melting point difference to assign the otherwise ambiguous stereochemistry of oximes. Our determination of the melting points of the *E* isomer (**3b**) was lower (115–119 °C) than that of the *Z* isomer (**3a**) (181–185 °C).

Inference can also be made based upon the crystallization timescale for each isomer. Following HPLC separation of the two stereoisomers of PUGNAc, we effected crystallization in the same manner as previously published studies involving only the active form of PUGNAc. In our hands, the *Z* isomer (**3a**) was noted to fully crystallize in 90 min. The *E* isomer (**3b**) took approximately 18 h to form crystals. This is in alignment with our supposition that all previous reports of PUGNAc involved exclusively *Z*-PUGNAc.

While these data are descriptive, ambiguity and disagreement are prevalent and physical trends such as melting points that are based upon the stereochemistry of the oxime will often be superseded due to the nature of the substrate as a whole. Thus, reliance on physical properties to ascertain the structure of these compounds is inadequate and often misleading. The far more compelling evidences lie within the numerous studies suggesting strong trends in the NMR spectral shifts of selected carbon and proton atoms within the structures of hydroximolactones and oximes. It is unfortunate that among the limited crystallographic data only one form (often the *Z* stereoisomer) of any given hydroximolactone structure exists so no direct correlation can be made between the absolute structure and significant NMR signals.^{7e}

The ¹H chemical shifts of the C2 methine protons for the *E* and *Z* isomers of PUGNAc have notable deviations in their chemical shifts. Precedence in similar oxime and hydroximolactone systems suggests that proximity to the oxygen of the oxime in the α -syn configuration will

de-shield the proton and cause a downfield shift in the signals of the *E*-isomer.⁸ However, this effect is largely dependent of the dihedral angle between the oxime oxygen and the C2 methine proton ($H-C-C=N-O-R$), and ambiguity based thereupon is plausible due to the assumed psuedochair conformations of the hydroximolactone. For example, studies have presented evidence of *E* hydroximolactones with C2-H shifts upfield of their *Z* counterparts.⁹ We were able to correctly identify the C2 methine proton through ¹H–¹H correlation NMR based upon coupling to the nitrogen proton of C2-NHAc group. The recorded ¹H signal for the C2-H carbon of the *Z* isomer (**3a**) was seen at 4.36–4.38 ppm and the corresponding signal of the *E* isomer (**3b**) was recorded at 4.62–4.64 ppm (Fig. 3), which are in agreement with the established trend. The chemical shifts seen, however, in the peracetylated compounds **6a** (4.78–80 ppm) and **6b** (4.71–4.73 ppm) are in conflict with the conventional precedent. It should be noted that the results for the deacetylated versions (**3a**, **3b**) are in alignment with several hydroximolactones presented by Vasella and co-workers.^{7e} Ultimately, ambiguity surrounding the accurate prediction of the deshielding effect for these molecules and the discrepancies between the recorded signals in this study and in other published work pressed us to rely on evidence other than the C2-H shifts.

The shifting of the C1 signal within the ¹³C spectrum of oximes can also be descriptive. The pattern is based upon steric compression and the observed trend suggests that within the more sterically compressed oxime the C1 signal will be shifted upfield.¹⁰ However, Sivertsen and co-workers show just the opposite for a small group of hydroximolactones.^{7b} The *E* and *Z* assignments of numerous hydroximolactones have since been made based solely on this study and the use of the ¹H C2-H spectral shift.^{7e,11} We observed that the C1 signals for the *E* form of PUGNAc (**3b**) (162.6 ppm) and the peracetylated PUGNAc (**6b**) (158.3 ppm) were shifted downfield relative to their *Z* counterparts (**3a**, **6a**) (158.8 ppm and 154.1 ppm, respectively) (Fig. 3). These observations are in alignment with the work of Siversten and co-workers but in direct conflict with the observation that the sterically compressed hydroximolactone will result in the upfield shift of C1.

Each of the aforementioned lines of evidence is suspect due to inconsistencies within the literature. However, our survey of the literature suggested that there is general agreement for the trends maintained for the C2 ¹³C NMR chemical shifts of hydroximolactone and oxime structures. Repeated studies show that the ¹³C signals of the α -syn carbon (C2) of oximes akin to the *E* stereoisomer of PUGNAc have a significant upfield shift relative to the α -anti-counterparts of the *Z* stereoisomer (Fig. 2). This is based upon steric compression (also called the γ effect) causing an upfield shift of the ¹³C nuclei in close proximity to a bulky moiety; in this case, the *N*-phenylcarbamate. This result was first described by Roberts and co-workers and Nelson and co-workers,¹² and numerous studies since have provided good precedence for this effect.¹³

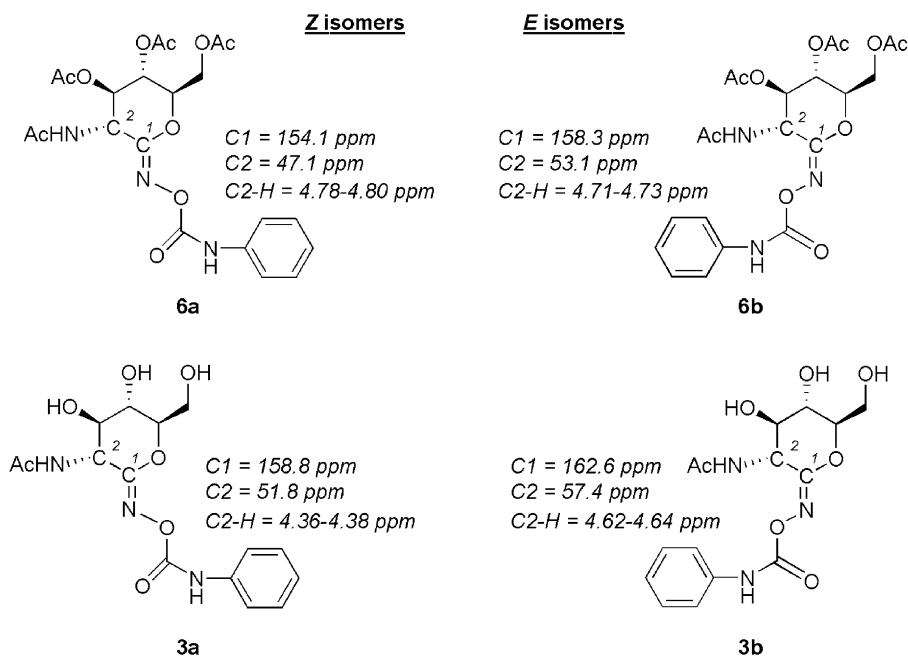


Figure 3. Selected NMR data; comparison of ^{13}C signals of C2 and comparison of ^1H signals of C2-H for *E* and *Z* PUGNac, and *E* and *Z* (OAc)₃PUGNac.

In our study, the correct assignment of the C2 carbon signals was accomplished by ^1H - ^{13}C correlation NMR based upon coupling to the methine C2 proton. The recorded ^{13}C signal for the C2 carbon of the *E* isomer (**3b**) was seen at 57.4 ppm and the corresponding signal of the *Z* isomer (**3a**) was recorded at 51.8 ppm (Fig. 3). This trend was also seen in the peracetylated compounds **6b** (53.1 ppm) and **6a** (47.1 ppm). Again, the ^{13}C shifts for C2 of the *E* and *Z* PUGNac and the peracetylated *E* and *Z* PUGNac are not in agreement with accepted precedence.

Based solely on the alignment of the NMR data with accepted trends it would be difficult to unambiguously assign the *E* and *Z* forms of PUGNac. The most compelling

line of evidence, however, is not precedence based upon NMR data (mostly based upon *oxime* precedence), but is the capability of only the *Z* isomer to undergo the Beckmann rearrangement (Fig. 4).¹⁴ It was initially noted that HPLC purification of the undefined mixture of the “F” and “S” isomers of PUGNac was complicated when, in a 0.1% trifluoroacetic acid aqueous buffer, the “F” isomer degraded over a period of 6–8 h. Following purification at neutral conditions, the “F” isomer was reevaluated within the acidic buffer conditions and the degradation products observed via LCMS. Two products were noted; one with a strong UV adsorption that maintained a mass of 136.2 and a second product with no associated chromophore that showed a mass of 220.1 (Fig. 5). These low resolution masses and their associated UV/vis signatures corre-

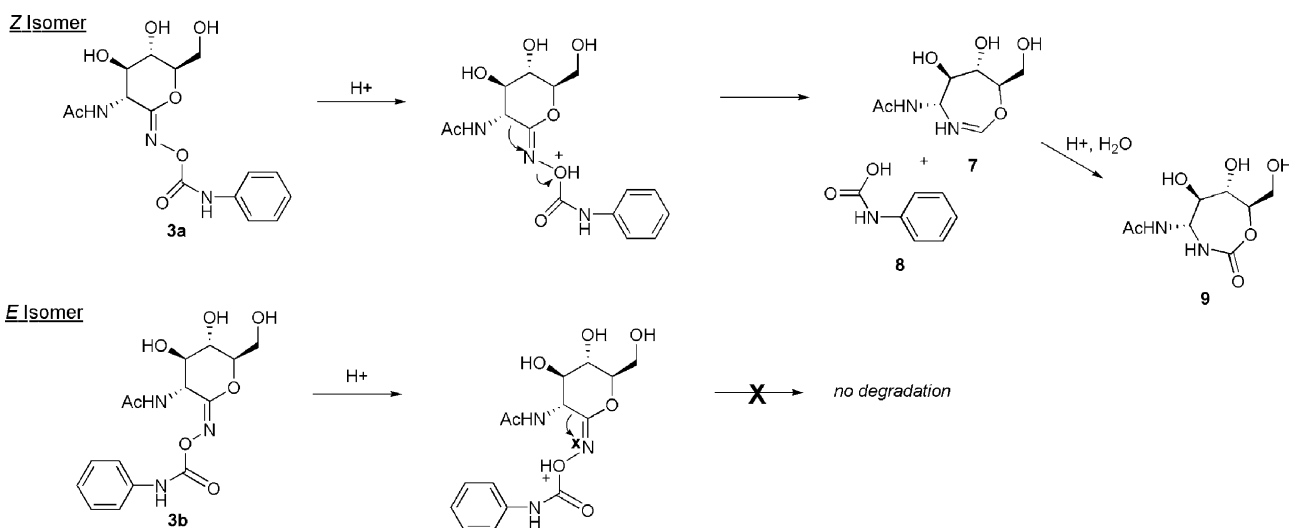
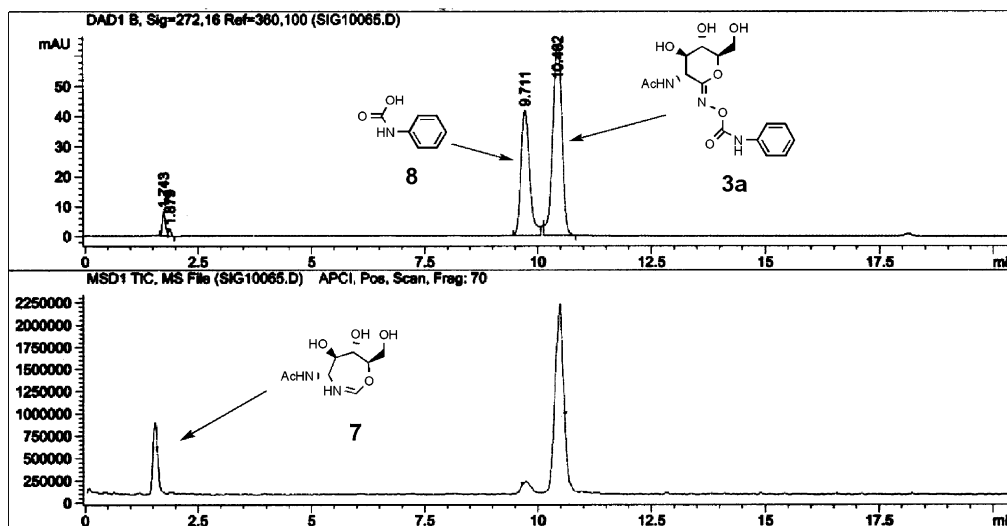


Figure 4. Description of the Beckmann rearrangement for *Z* PUGNac into **7**, **8**, and **9**.

Z Isomer @ 10 minutes



Z Isomer @ 80 minutes

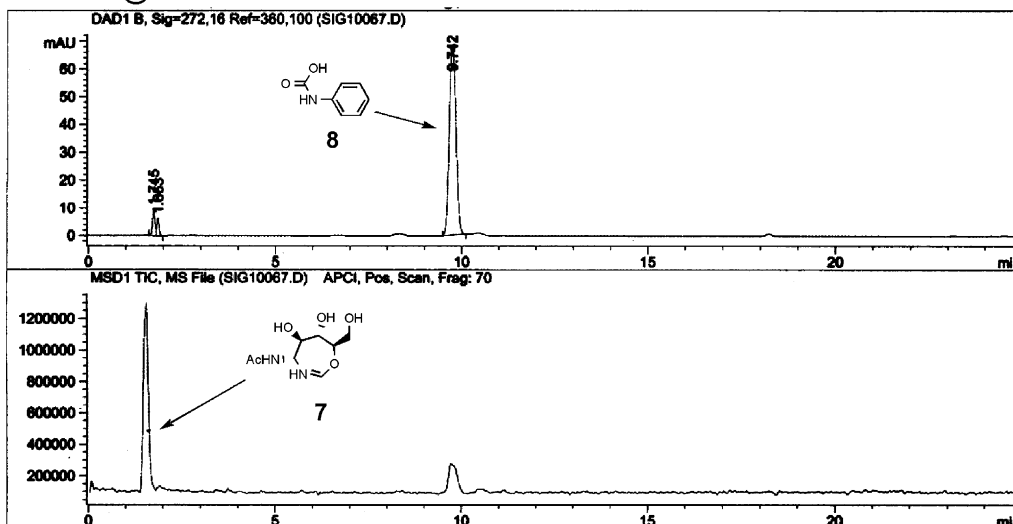


Figure 5. LCMS analysis of the rearrangement products of Z PUGNac in 0.1% TFA-buffered water within a linear gradient of increasing amounts of acetonitrile.

sponded well with the assumed products of the Beckmann rearrangement 7 ($m/z = 219.1$) and 8 ($m/z = 137.1$).

Following this observation, we tested the generality of rearrangement by exposing both isomers to several concentrations of trifluoroacetic acid. It was observed that the “S” isomer was stable up to and including exposure to a 50% trifluoroacetic acid solution. Conversely, the “F” isomer broke down at all trifluoroacetic acid concentrations tested. We next analyzed the products of the presumed Beckmann rearrangement via high resolution mass analysis and proton NMR. Following treatment of 8 mg of the “F” isomer with 25% trifluoroacetic acid in methanol, the resulting products were purified by HPLC. Analysis of the two products collected confirmed the existence of an aromatic compound with appropriate mass and proton NMR signals. The collection and analysis of the presumed sugar byproduct (7 or 9), observed as the non-hydrated product 7 via low resolution LCMS analysis, was complicat-

ed by the lack of fluorophore to allow diode array detection. A general collection based upon assumed retention times allowed for the collection of a compound with the appropriate low resolution mass and proton NMR signals for the non-hydrated product 7. Observation of the hydrated product (9) via mass analysis was not seen. It should be noted that the proton NMR we have observed could well represent products other than 7 including products formed via abnormal Beckmann rearrangements. We do not believe, however, that the existence of other Beckmann rearrangement type products alters our assignment of the stereochemistry of PUGNac.

With this evidence in hand, we returned to the original characterization of PUGNac by Vasella and co-workers to compare the NMR signatures of both the Z and E PUGNac (3a and 3b), and the Z and E acetylated versions (6a and 6b). It was confirmed that the ^1H and ^{13}C signals for both 3a and 6a corresponded well with the

published signals for PUGNac. The *E* PUGNac analogues **3b** and **6b**, however, had several significant deviations. Most notable were the observed signals for the C5-H multiplet of **6b**, which was shifted from 4.65–4.67 to 5.25–5.28, and the C6-H multiplet of **3b** that shifted from 3.76–3.78 to 4.53–4.55.

The characterization of the Beckmann rearrangement products of **3a** and good alignment of the NMR signals from our study to that of Vesella and co-workers have allowed us to unambiguously assign the “F” isomers with the *Z* stereochemical configuration.

2.2. Biological evaluation

With a satisfactory assignment of the *E* and *Z* stereoisomers of PUGNac complete, we concerned ourselves with the biochemical activities of each isomer. Both **3a** and **3b** were examined in the presence of recombinant *O*-GlcNAcase and ‘caged’ fluorogenic substrate, fluorescein di-*N*-acetyl- β -D-glucosaminide (FDGlcNAc) **10** (Fig. 6). We recently reported the action of *O*-GlcNAcase on **10** and the measurement of *O*-GlcNAcase activity based upon direct fluorescence measurement.¹⁵ The level of inhibition was determined based upon the quantification of fluorescence measured in the absence and presence of the PUGNac isomers (intensity of fluorescence was measured at $\lambda_{\text{ex}} = 485$ nm and at $\lambda_{\text{em}} = 535$ nm) (Fig. 6). The *Z* isomer of PUGNac (**3a**) was seen to strongly inhibit the action of *O*-GlcNAcase (approx 20% of *O*-GlcNAcase native activity in the presence of 1 μ M of **3a**), while the *E* isomer of PUGNac (**3b**) had a marked decrease in inhibition (approx 90% of *O*-GlcNAcase native activity in the presence of 1 μ M of **3b**).

We further examined the abilities of both the *E* and *Z* forms of PUGNac to evoke an increased incidence of *O*-GlcNAc incorporation upon proteins via methods previously reported by Philipsberg and co-workers.¹⁶ Treatment of separate cultures of both HEK and HeLa cells with aliquots of the peracetylated forms of *E* and *Z*

PUGNac (**6a** and **6b**) (from a stock ethanol solution diluted to a final concentration of 50 μ M) followed by incubation at 37 °C for 48 h and lysis of each culture and a control were followed by an analysis of *O*-GlcNAc integration via Western blot analysis. The peracetylated forms were utilized to achieve a more efficient cellular incorporation of each reagent and the ethanol treatment was mimicked within the control culture. The level of *O*-GlcNAc incorporation was quantified via infrared imaging of an IR-labeled *O*-GlcNAc specific antibody.

The *Z* form of the peracetylated PUGNac (**6a**) was noted to induce an approximately 1.4-fold increased level of *O*-GlcNAc incorporation upon proteins within the HeLa cell systems and similar results were found for HEK cells (Fig. 7 [gel B: lane 4 and gel D: lane 4]). The *E* isomer (**6b**), however, was seen to have no effect on *O*-GlcNAc levels (Fig. 7 [gel B: lane 3 and gel D: lane 3]). The experiments were repeated and the 1.4-fold increase was observed for a second time with the *Z* form, while the *E* form, again, produced no increased incidence of *O*-GlcNAc incorporation.

3. Discussion

The ability of the *Z* form of PUGNac to more potently inhibit the action of *O*-GlcNAcase relative to the *E* form is a significant finding. Consideration of the similarities of the PUGNac structure and the native substrate would strongly advocate a binding mechanism whereby the hydroximolactone *N*-acetyl triol moiety provides a significant portion of ligand recognition based upon substrate mimicry. Given that this moiety remains unchanged in both the *E* and *Z* forms of PUGNac, we may well envision a mechanism of enzyme inhibition by *Z* PUGNac that is moderately tenuous.

It is worth noting that PUGNac has been viewed within the crystallographic analysis of glycogen phosphorylase b

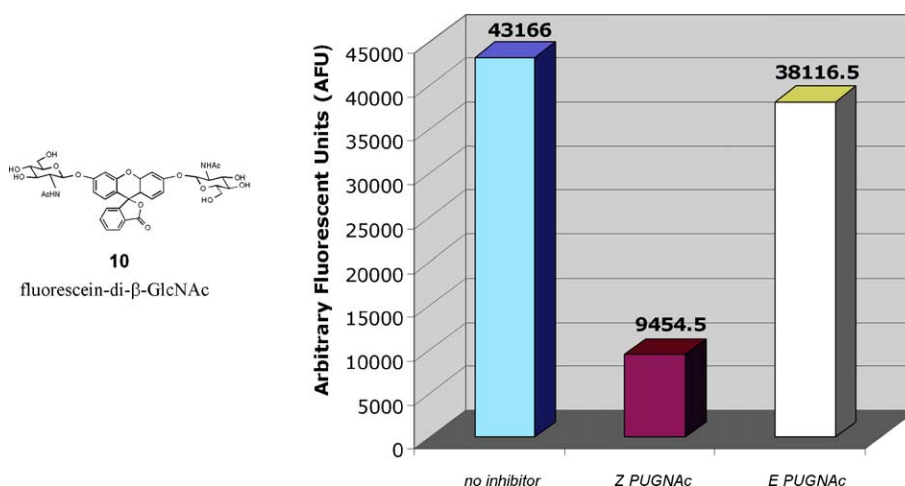


Figure 6. Structure of fluorescein-di- β -GlcNAc (**10**) and activity of *O*-GlcNAcase based upon fluorescence: (1) control—no inhibitor, (2) with 1.0 μ M *Z*-PUGNac (**3a**), and (3) with 1.0 μ M *E*-PUGNac (**3b**).

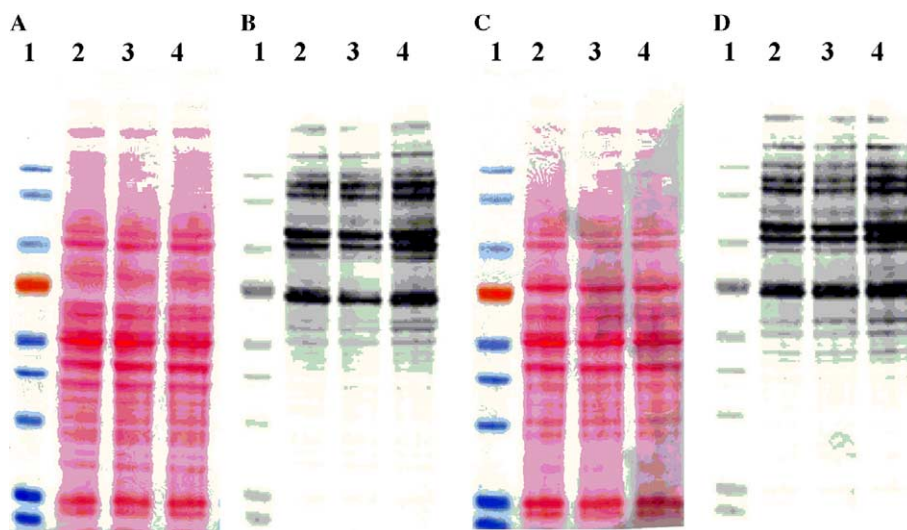


Figure 7. Effect of the oxime stereochemistry of PUGNAC on protein incorporation of *O*-GlcNAc. Ponceau S staining of the nitrocellulose membranes (gels A and C) reveals equivalent proteins were loaded. Western blot proteins from HeLa (gel B) and HEK (gel D) indicate an increased incidence of *O*-GlcNAc protein incorporation. Lane 1, protein marker; lanes 2–4, proteins from cells cultured for 48 h in the absence of inhibitor and presence of 50 mM *E*-(OAc)₃-PUGNAC (**6b**) and *Z*-(OAc)₄-PUGNAC (**6a**), respectively. IR quantification revealed an approximately 1.4-fold increase in *O*-GlcNAc incorporation upon proteins when both HeLa and HEK cells were treated with *Z*-(OAc)₃-PUGNAC (**6a**) (gel B—lane 4 and gel D—lane 4, respectively).

and was seen to exist as the *Z* stereoisomer.¹⁷ However, a compound similar to PUGNAC (*N,N'*-diacetyl-chitobionoxime-*N*-phenylcarbamate (HM508)) was recently viewed within the crystallographic analysis of ChiB as the *E* stereoisomer.¹⁸ The exact ligand–enzyme docking arrangement for *Z* PUGNAC and *O*-GlcNAcase is worth further exploration.

Structural activity relationships based solely on stereochemistry are widespread throughout medicinal chemistry and in modern drug discovery.¹⁹ Recent reports, including observations of the stereospecific antitumor activity of a radicicol oxime analogue and the stereospecific agonistic activity of oxime-piperidine derivatives at the CCR5 receptor, demonstrate that oxime stereochemistry can be an important mediator of structure and function.²⁰

The assignment of stereochemistry within *E* and *Z* oximes and/or hydroximolactones can be deceptive. The methods utilized to delineate between the two stereoisomers has evolved from simple qualitative analyses to, in the best case scenario, crystallographic methods. Herein, we describe how both qualitative methods and NMR signal comparison can be misleading. Further, the *E* and *Z* isomers of PUGNAC represent important counter-examples to several of the relied upon NMR methods to predict oxime stereochemistry.

The understanding that PUGNAC relies on the correct oxime stereochemistry to potently inhibit *O*-GlcNAcase compels us to reconsider of the means of inhibition by *Z* PUGNAC and the mechanism of action of *O*-GlcNAcase. Certainly, the fundamentally different shapes of the two stereoisomers will have reverberations in the binding ability of *E* and *Z* PUGNAC to *O*-GlcNAcase and ultimately their inhibitory potential. Clearly, the *Z*

isomer binds in a manner that better positions the *N*-phenylcarbamate moiety in terms of ligand–enzyme contacts and steric accommodation.

Further, a recent report²¹ and congruent observations in our own laboratory²² have noted the success of a GlcNAc-thiazoline as a potent inhibitor of *O*-GlcNAcase. The success of this analogue as an inhibiting agent would suggest that a substrate assisted mechanism (Fig. 8) is being utilized by *O*-GlcNAcase and that obstruction of such an enzymatic mechanism is a key necessity for small molecule inhibitors like PUGNAC.²³ The positioning of the *N*-acetyl group and the reactivity of anomeric ether linkage are both imperative to this type of mechanism. The oxime component of both *E* and *Z* PUGNAC would likely block any such intermediate from forming and any inhibition enhancement of the *Z* form seems unlikely to be based upon this possible substrate–enzyme interaction. The enhanced potency of *Z*-PUGNAC might indicate that the positioning of the *N*-acetyl group is a key binding motif based upon the assumed steric clash of this moiety with the phenyl carbamate in the *E*-PUGNAC form (Fig. 8). Clearly, visualization of the active form of PUGNAC within the active site of *O*-GlcNAcase would resolve many of these questions and allow for refinement of *Z*-PUGNAC into a more specific and potent enzyme inhibitor.

4. Conclusion

Herein, we report that the inhibition of *O*-GlcNAcase by PUGNAC is highly dependent on the stereochemical configuration of the oxime portion of the PUGNAC chemical structure. Further, through experimental evidence, primarily the observation that the *Z* stereoisomers will undergo the Beckmann rearrangement, we

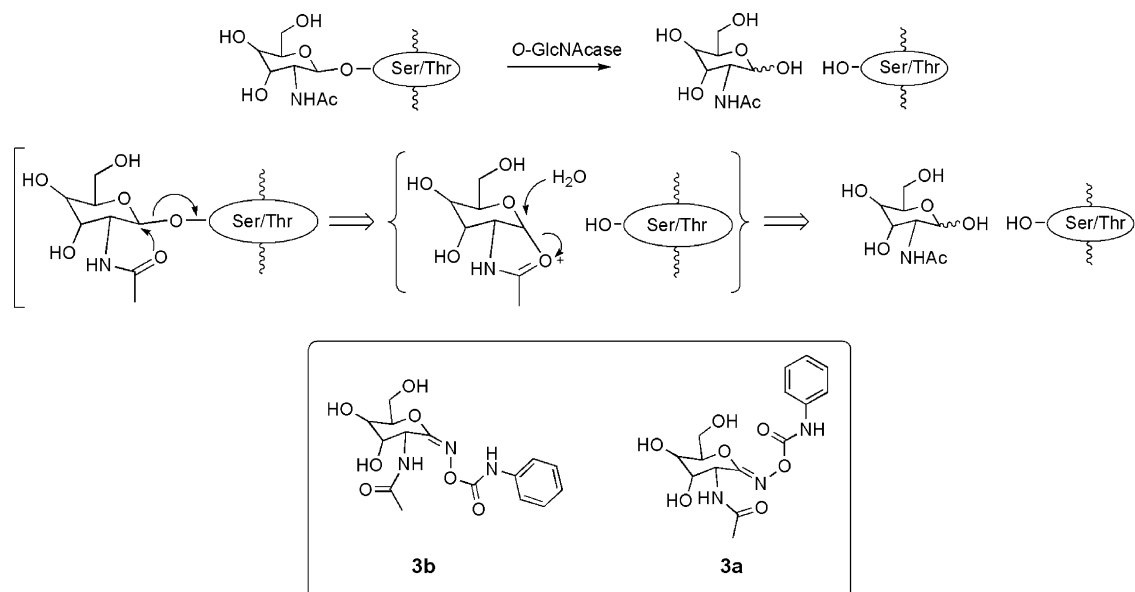


Figure 8. Example of substrate assisted mechanism and structural comparison of *E* and *Z* PUGNAc.

have shown that the *Z* form of PUGNAc is the active isomer. Importantly, only the *Z* form of PUGNAc was shown to amplify the incorporation of *O*-GlcNAc on proteins within both HeLa and HEK cell systems.

5. Experimental

5.1. General

The synthetic elaboration was done in an identical fashion as reported in Ref. 6b. ^1H NMR data were recorded on a Varian Gemini300, and ^{13}C NMR and COSY data were recorded on a Bruker 600. Spectra were recorded in d_6 -DMSO and/or D_2O and were referenced to the residual solvent peak at 2.50 and 4.79, respectively. Reverse-phase (C18) HPLC was carried out using an Agilent HPLC with a ZorbaxTM SP-C18 semi-prep column. All melting points were determined with a Thomas-Hoover apparatus and are uncorrected. High-resolution mass spectroscopy measurements were performed on a Micromass/Waters LCT Premier Electrospray TOF mass spectrometer.

5.2. *O*-(2-Acetamido-3,4,5-tri-*O*-acetyl-*D*-glucopyranosylidene)amino-*Z*-*N*-phenylcarbamoyl (6a)

Synthesis was accomplished in an identical fashion and with equivalent yields as in Ref. 6b. Following purification of the isomer mixture via flash chromatography, an aliquot was removed for HPLC separation of the isomers. HPLC purification was achieved using a linear gradient of water containing increasing amounts of CH_3CN (0 \rightarrow 15 min, linear gradient from 30% to 60% CH_3CN at a flow rate of 4 mL/min; R_t 9.6 min). The triacetyl-*Z*-PUGNAc (6a) was obtained as a white solid following lyophilization. ^1H NMR (d_6 -DMSO): δ 1.87 (s, 3H), 2.00 (s, 3H), 2.03 (s, 3H), 2.05 (s, 3H), 4.19–4.21 (m, 1H), 4.37–4.40 (m, 1H), 4.65–4.67 (m, 1H),

4.78–4.80 (m, 1H), 5.22–5.26 (m, 1H), 5.33–5.36 (m, 1H), 7.02–7.05 (m, 1H), 7.29–7.32 (m, 2H), 7.48–7.49 (m, 2H), 8.61 (d, $J_{\text{HH}} = 7.68$ Hz, 1H), 9.74 (s, 1H); ^{13}C NMR (d_6 -DMSO): δ 18.8, 18.1, 18.9, 20.9, 47.1, 60.0, 65.5, 69.3, 74.2, 117.3, 121.4, 127.2, 136.8, 149.8, 154.1, 167.5, 167.7, 168.0, 168.4; mass spectrometry (TOF); $m/z = 480.1603$ (M+H) (theoretical 480.1613).

5.3. *O*-(2-Acetamido-3,4,5-tri-*O*-acetyl-*D*-glucopyranosylidene)amino-*E*-*N*-phenylcarbamoyl (6b)

Synthesis was accomplished in an identical fashion and with equivalent yields as in Ref. 6b. Following purification of the isomer mixture via flash chromatography, an aliquot was removed for HPLC separation of the isomers. HPLC purification was achieved using a linear gradient of water containing increasing amounts of CH_3CN (0 \rightarrow 15 min, linear gradient from 30% to 60% CH_3CN at a flow rate of 4 mL/min; R_t 10.2 min). The triacetyl-*E*-PUGNAc (6b) was obtained as a white solid following lyophilization. ^1H NMR (d_6 -DMSO): δ 1.90 (s, 3H), 1.99 (s, 3H), 2.04 (s, 3H), 2.05 (s, 3H), 4.12–4.15 (m, 1H), 4.54–4.57 (m, 1H), 4.71–4.73 (m, 1H), 5.14–5.17 (m, 1H), 5.25–5.28 (m, 1H), 5.34–5.35 (m, 1H), 7.02–7.04 (m, 1H), 7.28–7.31 (m, 2H), 7.47–7.48 (m, 2H), 8.90 (d, $J_{\text{HH}} = 7.56$ Hz, 1H), 9.84 (s, 1H); ^{13}C NMR (d_6 -DMSO): δ 18.9, 19.0, 20.7, 53.1, 60.4, 65.3, 72.2, 80.0, 117.6, 121.4, 127.2, 136.9, 149.8, 158.3, 167.3, 167.5, 167.7, 168.6; mass spectrometry (TOF); $m/z = 480.1617$ (M+H) (theoretical 480.1613).

5.4. *O*-(2-Acetamido-2-deoxy-*D*-glucopyranosylidene)amino-*Z*-*N*-phenylcarbamoyl (3a)

Synthesis was accomplished in an identical fashion as in Ref. 6b. Following removal of the solvent by rotary evaporation, the crude product mixture was purified by HPLC without further workup. HPLC purification was achieved using a linear gradient of water containing

increasing amounts of CH₃CN (0 → 15 min, linear gradient from 10% to 25% CH₃CN at a flow rate of 4 mL/min; *R*_t 12.6 min). Z-PUGNAc (**3a**) was obtained as a white solid following lyophilization. Crystallization of a 20 mg aliquot of the sample was achieved in a solution of methanol/ethyl acetate/hexanes (10 mL:30 mL:30 mL). Crystals formed in approximately 90 min. Mp 181–185 °C. ¹H NMR (*d*₆-DMSO): δ 1.89 (s, 3H), 3.56–3.69 (m, 3H), 3.76–3.78 (m, 1H), 3.93–3.95 (m, 1H), 4.36–4.38 (m, 1H), 4.94 (br s, 1H), 5.59 (br s, 2H), 7.01–7.03 (m, 1H), 7.27–7.30 (m, 2H), 7.48–7.49 (m, 2H), 8.33 (d, *J* = 7.98 Hz, 1H), 9.59 (s, 1H); ¹³C NMR (D₂O at 15 °C): δ 23.8, 51.8, 60.7, 69.2, 72.9, 83.1, 119.3, 123.5, 129.4, 139.2, 152.4, 158.8, 169.9; mass spectrometry (TOF); *m/z* = 354.1289 (M+H) (theoretical 354.1296).

5.5. *O*-(2-Acetamido-2-deoxy-*D*-glucopyranosylidene)amino-*E*-*N*-phenylcarbamoyl (**3b**)

Synthesis was accomplished in an identical fashion as in Ref. 6b. Following removal of the solvent by rotary evaporation, the crude product mixture was purified by HPLC without further workup. HPLC purification was achieved using a linear gradient of water containing increasing amounts of CH₃CN (0 → 15 min, linear gradient from 10% to 25% CH₃CN at a flow rate of 4 mL/min; *R*_t 14.5 min). *E*-PUGNAc (**3b**) was obtained as a white solid following lyophilization. Crystallization of a 30 mg aliquot of the sample was achieved in a solution of methanol/ethyl acetate/hexanes (10 mL:30 mL:30 mL). Crystals formed in approximately 18 h. Mp 115–119 °C. ¹H NMR (*d*₆-DMSO): δ 1.87 (s, 3H), 3.50–3.53 (m, 1H), 3.67–3.69 (m, 1H), 3.83–3.86 (m, 1H), 4.11–4.12 (m, 1H), 4.53–4.55 (m, 1H), 4.62–4.64 (m, 1H), 4.69 (br s, 1H), 5.03 (br s, 1H), 5.92 (br s, 1H), 7.00–7.03 (m, 1H), 7.27–7.30 (m, 2H), 7.48–7.49 (m, 2H), 8.66 (d, *J* = 7.74 Hz, 1H), 9.73 (br s, 1H); ¹³C NMR (*d*₆-DMSO): δ 23.1, 57.4, 63.6, 68.8, 73.3, 86.0, 119.4, 123.5, 129.4, 139.2, 152.3, 162.6, 169.5; mass spectrometry (TOF); *m/z* = 354.1316 (M+H) (theoretical 354.1296).

5.6. Beckmann rearrangement product characterization

To a solution of methanol and trifluoroacetic acid (3 mL MeOH:1 mL TFA) was added **3a** (8 mg, 0.022 mmol) and the resulting solution was allowed to stir for 10 min at room temperature. Solvent was removed under reduced pressure and the reaction mixture was dissolved in 2 mL of a 1:1 mixture of acetonitrile and water. HPLC purification was achieved using a linear gradient of water containing increasing amounts of CH₃CN (0 → 10 min, linear gradient from 10% to 80% CH₃CN at a flow rate of 4 mL/min). Time of retention for **8** was 5.1 min. Compound **8** ¹H NMR (*d*₆-DMSO): δ 6.97–7.04 (m, 1H), 7.23–7.38 (m, 2H), 7.42–7.53 (m, 2H); mass spectrometry (TOF); *m/z* = 137.0444 (M+) (theoretical 137.0476) and *m/z* = 179.0759 (M+CH₃CN) (theoretical 179.0820). Time of retention for **7** was 1.16 min. Compound **7** ¹H NMR (*d*₆-DMSO): δ 1.86 (s, 3H), 3.22–3.24 (m, 1H), 3.41–3.44 (m, 1H), 3.55–

3.57 (m, 1H), 3.89–3.95 (m, 1H), 4.13–4.16 (m, 1H) 7.57–7.59 (s, 1H).

5.7. Expression and purification of recombinant *O*-GlcNAcase

Cultures of TOP 10 cells containing pBAD/HisA human *O*-GlcNAcase clone expression vector were grown overnight in Luria–Bertani (LB) broth (Difco) supplemented with ampicillin (50 µg/ml). Induction of *O*-GlcNAcases was initiated by adding arabinose solution (0.02%) when the OD₆₀₀ of cultures reached around 0.5. The cultures were further grown for 4 h at 30 °C at 200 rpm. The cells were harvested by centrifugation at 4000g for 15 min in a Sorvall® RC 5C Plus (DuPont) centrifuge. The pellet was subjected to freeze–thaw and suspended in 1/50 of the original volume in 0.1 mg/ml lysozyme, 20 mM Tris–HCl, pH 8.0, 1 mM DTT, 0.1% Triton X-100, and an EDTA-free protease inhibitor cocktail tablet (1 tablet/10 ml). The suspension was incubated at room temperature for 5 min and the lysate was sonicated on ice (4 × 10 s, setting 3, Misonix Ultrasonic Processor). The supernatant was obtained after centrifugation at 20,000g for 15 min. Expressed His₆-tagged *O*-GlcNAcase in the supernatant was purified on His-Trap HP column (Amersham Biosciences) using the slightly modified manufacturer's protocol. Fractions (1 ml) collected throughout the separation were assayed for protein (absorbance at 280 nm) and were further assayed for *O*-GlcNAcase activity according to the protocol described below. Fractions showing enzyme activity were pooled and concentrated using a Centricon 100 microconcentrator (Amicon). Pierce BCA protein assay reagent was used to estimate protein concentration. Purity of *O*-GlcNAcase was confirmed by Ponceau S staining of the membrane (Sigma) and Western blot analysis using anti His-Tag antibody (Abcam).

5.8. *O*-GlcNAcase's enzymatic assay

Four microliters of purified recombinant *O*-GlcNAcase was incubated in 0.1 M citrate/phosphate buffer, pH 6.5, containing 30 µM of the fluorogenic substrate (**10**), in a final volume of 100 µl in the presence of 1 µM of inhibitors (**3a** and **3b**) and in the absence of the inhibitor at 37 °C for 30 min. The assays were terminated by adding 900 µl of 0.5 M Na₂CO₃ solution. Two hundred microliters of assay solution was transferred into a 96-well plate and fluorescence was measured at the excitation wavelength of 485 nm and at the emission wavelength of 535 nm on the Wallac 1420 fluorometer.

5.9. Cell culture and inhibition

HEK and HeLa cells were cultured in a DMEM (Gibco) supplemented with 10% FBS (Invitrogen). Aliquots of inhibitors (**6a** and **6b**) in a 50 µL of a stock in 100% ethanol were delivered into 10 mL tissue culture flasks to yield a final concentration of 50 µM of inhibitor and the ethanol was evaporated. The cells were incubated in humidified 95% air and 5% CO₂ at 37 °C for 48 h. Cells were harvested and were pooled by centrifugation (200g, 5 min). Cells were washed twice with PBS, pH 7.0

(10 mL) and pelleted (200g, 5 min). A culture of control cells was treated in the same manner as above, except that aliquots of ethanol were delivered into the tissue culture flask and the ethanol was evaporated and the cultures contained no inhibitors.

5.10. Western blot analysis

The pellet was suspended in 0.8 mL lysis buffer containing 20 mM Tris–HCl, pH 8.0, 1 mM DTT, 0.1% Triton X-100, and an EDTA-free protease inhibitor cocktail (1 tablet/10 mL). The suspension was incubated at room temperature for 5 min and sonicated on ice (4 × 10 s, setting 3, Misonix Ultrasonic Processor). The supernatant was obtained after centrifugation at 20,000g for 15 min. Pierce BCA protein assay reagent was used to estimate protein concentration. Samples were loaded onto a 4–12% Nu-PAGE pre-cast gel and proteins were separated by electrophoresis and then transferred to a nitrocellulose membrane for immunoblotting. The blot was probed with *O*-GlcNAc specific antibody RL2 (mouse IgG1, Affinity Bioreagents, Inc.) at 1:1000 dilution and infrared (IR)-labeled anti-mouse IgG Goat antibody (Rockland, Inc.). The blot was scanned on the Odyssey Infrared Imager (LI-COR Biosciences). Relative intensity of *O*-GlcNAc level was quantitated using the Odyssey Infrared Imaging System application software.

Acknowledgments

The authors thank Kenneth A. Jacobson for helpful discussions during the preparation of this manuscript. Appreciation is also expressed to Victor Livengood and Sonya Hess for assistance in obtaining the HRMS data. We gratefully acknowledge the support of the NIH Intramural Research Program.

References and notes

- (a) Comer, F. I.; Hart, G. W. *J. Biol. Chem.* **2000**, *275*, 29179; (b) Wells, L.; Vosseller, K.; Hart, G. W. *Science* **2001**, *291*, 2376; (c) Wells, L.; Hart, G. W. *FEBS Lett.* **2003**, *546*, 154.
- (a) Hanover, J. A. *FASEB J.* **2001**, *15*, 1865; (b) Zachara, N. E.; Hart, G. W. *Chem. Rev.* **2002**, *102*, 431; (c) Slawson, C.; Hart, G. W. *Curr. Opin. Struct. Biol.* **2003**, *13*, 631.
- Konrad, R. J.; Zhang, F.; Hale, J. E.; Knierman, M. D.; Becker, G. W.; Kudlow, J. E. *Biochem. Biophys. Res. Commun.* **2002**, *293*, 207.
- (a) Horsch, M.; Hoesch, L.; Vasella, A.; Rast, D. M. *Eur. J. Biochem.* **1991**, *197*, 815; (b) Dong, D. L.-Y.; Hart, G. W. *J. Biol. Chem.* **1994**, *269*, 19321; (c) Konrad, R. J.; Mikolaenko, I.; Tolar, J. F.; Liu, K.; Kudlow, J. E. *Biochem. J.* **2001**, *356*, 31.
- Arias, E. B.; Kim, J.; Cartee, G. D. *Diabetes* **2004**, *53*, 921.
- (a) Beer, D.; Maloisel, J.-L.; Rast, D. M.; Vasella, A. *Helv. Chim. Acta* **1990**, *73*, 1918; (b) Mohan, H.; Vasella, A. *Helv. Chim. Acta* **2000**, *83*, 114.
- (a) Johnson, J. E.; Springfield, J. R.; Hwang, J. S.; Hayes, L. J.; Cunningham, W. C.; McClaugherty, D. L. *J. Org. Chem.* **1971**, *36*, 284; (b) Kjaer, A.; Larson, I. K.; Sivertsen, P. *Acta Chem. Scand. Ser. B* **1977**, *31*, 415; (c) Bradshaw, J.; Webb, G. B. U.S. Patent # 3903113, 1975.(d) Aebischer, B. M.; Hanseen, H. W.; Vasella, A. T.; Schweizer, W. B. *J. Chem. Soc. Perkin Trans. 1* **1982**, 2139; (e) Beer, D.; Vasella, A. *Helv. Chim. Acta* **1985**, *68*, 2254; (f) Kim, H. Y.; Lantrip, D. A.; Fuchs, P. L. *Org. Lett.* **2001**, *3*, 2137.
- (a) Baji, H.; Flammang, M.; Kimny, T.; Gasquez, F.; Compagnon, P. L.; Delcourt, A. *Eur. J. Med. Chem.* **1995**, *30*, 617; (b) Emami, S.; Shafiee, A. *Heterocycles* **2001**, *55*, 2059.
- Uhlmann, P.; Harth, E.; Naughton, A. B.; Vasella, A. *Helv. Chim. Acta* **1994**, *77*, 2335.
- Gordon, M. S.; Sojka, S. A.; Krause, J. G. *J. Org. Chem.* **1984**, *49*, 97.
- (a) Takahashi, Y.; Vasella, A. *Helv. Chim. Acta* **1992**, *75*, 1563; (b) Vasella, A.; Witzig, C.; Waldraff, C.; Uhlmann, P.; Briner, K.; Bernet, B.; Panza, L.; Husi, R. *Helv. Chim. Acta* **1993**, *76*, 2847.
- (a) Levy, G. C.; Nelson, G. L. *J. Am. Chem. Soc.* **1972**, *94*, 4897; (b) Hawkes, G. E.; Herwig, K.; Roberts, J. D. *J. Org. Chem.* **1974**, *39*, 1017.
- (a) Unterhalt, B.; Koehler, H. *Archiv. Der Pharmazie* **1978**, *311*, 366; (b) Khouri, N.; Usubillaga, A.; Delgado, J. N. *Spectrosc. Lett.* **1993**, *26*, 859; (c) Sohar, P.; Bodor, A.; Schwartz, R. *Steroids* **1999**, *64*, 246; (d) Afonin, A. V.; Ushakov, I. A.; Tarasova, O. A.; Shmidt, E. Y.; Mikhaleva, A. I.; Voronov, V. K. *Russ. J. Org. Chem.* **2000**, *36*, 1777; (e) Holzer, W.; Hahn, K.; Brehmer, T.; Claramunt, R. M.; Perez-Torralla, M. *Eur. J. Org. Chem.* **2003**, 1209.
- Nguyen, M. T.; Raspoet, G.; Vanquickenborne, L. G. *J. Am. Chem. Soc.* **1997**, *119*, 2552.
- Kim, E.-J.; Kang, D. O.; Love, D. C.; Hanover, J. A. *Biochemistry*, submitted.
- Haltiwanger, R. S.; Grove, K.; Philipsberg, G. A. *J. Biol. Chem.* **1998**, *273*, 3611.
- Barford, D.; Schwabe, J. W. R.; Oikonomakos, N. G.; Acharya, K. R.; Hajdu, J.; Papageorgiou, A. C.; Martin, J. L.; Knott, J. C. A.; Vasella, A.; Johnson, L. N. *Biochemistry* **1988**, *27*, 6733.
- Vaaje-Kolstad, G.; Vasella, A.; Peter, M. G.; Netter, C.; Houston, D. R.; Westereng, B.; Synstad, B.; Eijsink, V. G. H.; van Aalten, D. M. F. *J. Biol. Chem.* **2004**, *279*, 3612.
- Agranat, I.; Craner, H.; Caldwell, J. *Nat. Rev. Drug Disc.* **2002**, *1*, 753.
- (a) Soga, S.; Sharma, S. V.; Shiotsu, Y.; Shimizu, M.; Tahara, H.; Yamaguchi, K.; Ikuina, Y.; Murakata, C.; Tamaoki, T.; Kurebayashi, J.; Schulte, T. W.; Neckers, L. M.; Akinaga, S. *Cancer Chemother. Pharmacol.* **2001**, *48*, 435; (b) Palani, A.; Shapiro, S.; Josien, H.; Bara, T.; Clader, J. W.; Greenlee, W. J.; Cox, K.; Strizke, J. M.; Baroudy, B. M. *J. Med. Chem.* **2002**, *45*, 3143.
- Macauley, M. S.; Whitworth, G. E.; Debowski, A. W.; Chin, D.; Voadlo, E. J. *J. Biol. Chem.* **2005**, *280*, 25313.
- Kim, E.-J.; Darout, E.; Thomas, C. J.; Knapp, S.; Hanover, J. A. manuscript in preparation.
- Tews, I.; Terwisscha van Scheltinga, A. C.; Perrakis, A.; Wilson, K. S.; Dijkstra, B. W. *J. Am. Chem. Soc.* **1997**, *119*, 7954.